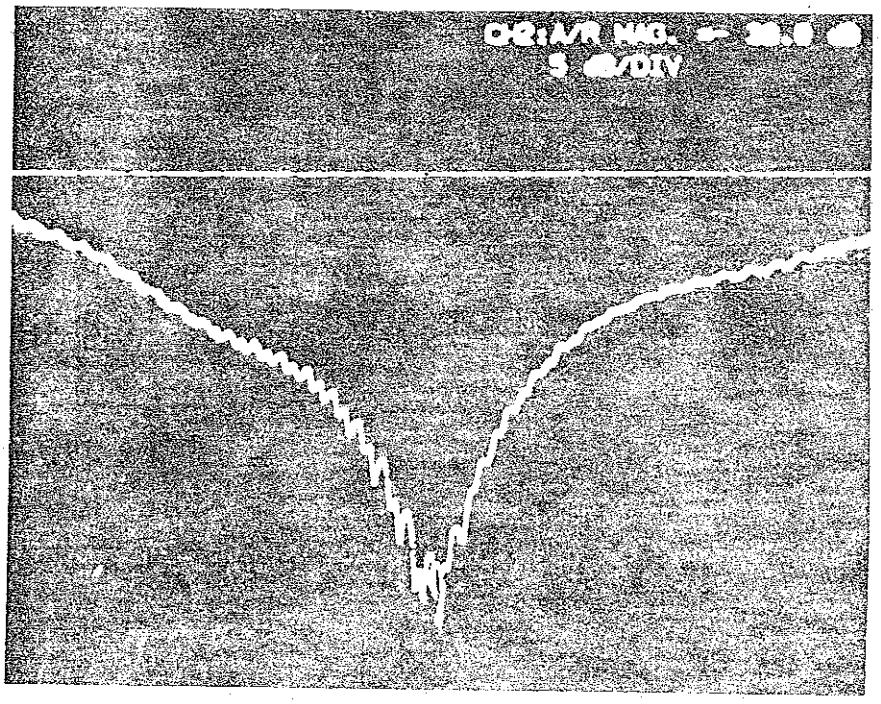

Fig.2—9.Magnitude of the reflection coefficient of the transducer No.1 in rectangular coordinates. The horizontal scale is frequency centered at 553 MHz with scan width f=40MHz. The frequency difference between any two adjacent ripples is determined to be 0.58 MHz.

In our case, we take v=7300m/s and d=3.1mm in Eq.(2—40), the results just conform with the experiments.

From Fig.2—9 we can see that the ripples can be divided into two parts, one is much stronger than the other. The two are arranged one by one alternately. Here we consider that two echo signals have been detected. Since the first one is stronger, so is the interference.

C.The periodicity of the ASL

As mentioned before, the ASL can be viewed as composed of a series of sound δ-sources. By the action of an electric δ pulse, each individual sound source will launch a sound δ pulse. Then these sound pulses will be transmitted into the transmission medium one by one. The time interval between any two sound pulses is determined by the spatial interval of their sound sources. The time interval and the spatial interval differ from each other by a proportional factor v, the velocity of the sound wave. Thus from v_S=3600m/s and the value of the time interval determined in §2—2 t=3.66ns, the periodicity of the ASL can be estimated, which is 13.2μm, the same as the value measured by optical microscope.

D.Power flow density in the transmission medium

The transducer discussed here can be used in many ways such as acoustic delay lines, acoustooptic deflectors, acoustooptic modulators etc. In applications of acoustooptic devices, the intensity of the diffracted light is directly proportional to the acoustic power. Therefore it is worth while discussing the power flow density emitted by the ASL.

First we must derive the acoustic Poynting vector which, in our case, is

$$\vec{P}=-\vec{v}\cdot\vec{\vec{T}}=-v_3T_3\hat{k}. \qquad (2—42)$$

Here v_3 is the velocity of the particle in vibration, $\hat{k}$ is a unit vector along the z-axis and

$$T_3=-\frac{1}{2}jke^{j(\omega t-kz)}\int h_{33}(z')D_3(z')e^{jkz'}dz'$$

$$=-2h_{33}D_3\frac{\sin[\frac{1}{2}kN(a+b)]}{\sin[\frac{1}{2}k(a+b)]}\left\{[\cos\frac{1}{2}k(a-b)-\cos\frac{1}{2}k(a+b)]\cos\frac{1}{2}kN(a+b)\right.$$

$$\left.-\sin\frac{1}{2}k(a-b)\sin\frac{1}{2}kN(a+b)\right\}e^{j(\omega t-kz)}, \quad (2—43)$$

In obtaining Eq.(2—43), both real-sources and image-sources are included.

v_3 can be obtained from

$$\partial T_3/\partial z=\rho\partial^2U_3/\partial t^2=\rho\partial v_3/\partial t\ , \quad (2—44)$$

which is

$$v_3=-\frac{v}{C_{33}^D}T_3\ , \quad (2—45)$$

Neglecting the exponential term, we have

$$\vec{p}=\hat{k}\frac{4h_{33}^2D_3^2v}{C_{33}^D}\left\{\frac{\sin\frac{1}{2}kN(a+b)}{\sin\frac{1}{2}k(a+b)}\right\}^2\left\{[\cos\frac{1}{2}k(a-b)-\cos\frac{1}{2}k(a+b)]\right.$$

$$\left.\times\cos\frac{1}{2}kN(a+b)-\sin\frac{1}{2}k(a-b)\sin\frac{1}{2}kN(a+b)\right\}^2, \quad (2—46)$$

The power flow density is then expressed as

$$P=\vec{p}\cdot\hat{k}\ . \qquad (2\text{—}47)$$

In order to gain an insight into the merit of the ASL, let us consider a special case of a=b. Eq.(2—47) becomes

$$P=-\frac{4h_{33}^2D_3^2v}{C_{33}^D}\left\{\frac{\sin(kNa)}{\cos\frac{1}{2}ka}\right\}^2\sin^2(\tfrac{1}{2}ka)\cos^2kNa. \qquad (2\text{—}48)$$

At resonance, i.e., $\frac{1}{2}ka=\pi/2$,

$$P=4(2N)^2\frac{h_{33}^2D_3^2v}{C_{33}^D}\ . \qquad (2\text{—}49)$$

If the transducer is made of only one domain, that is, N=1 and b=0, then we have

$$P=4\frac{h_{33}^2D_3^2v}{C_{33}^D}\ . \qquad (2\text{—}50)$$

Comparing with that of the ASL, we find that the power flow density of the ASL is proportional to the square of the domain numbers. This shows that with the transducer made of an ASL, the power flow density in the transmission medium can be greatly increased. This conclusion is very useful in practical applications.

E.Something more about the transducer

An inspection of Eqs.(2—17) and (2—24) shows that if we exchange the positions of a and b, the results are quite

different for different cases: Eq.(2—17)(for resonators) remains the same, while Eq.(2—24) (for transducers) are changed. Physically, these results arise from the different boundary conditions of resonators and transducers. In order to explain these results more clearly, we will resort to Figs.10 and 11. According to our derivation, Eqs.(2—17) and (2—24) are valid for the situations of Fig.2—10(a) and Fig.2—11(a), respectively. The permutation of a and b in Eqs.(2—17) and (2—24) is equivalent to transform the

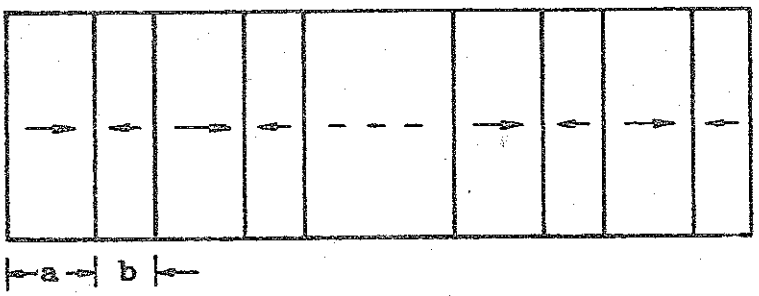

(a)

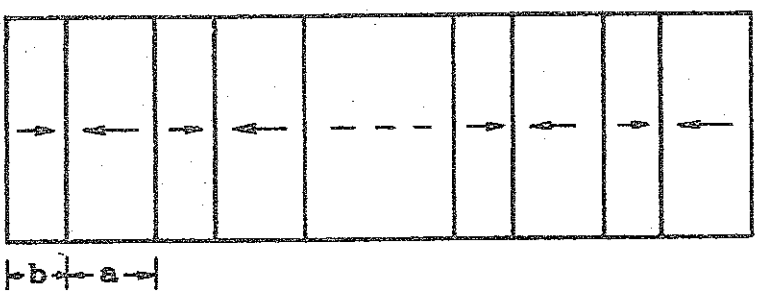

(b)

Fig.2—10.Schematic diagrams of resonators made of ASL(electrodes are omitted). Domains with their polarization directions towards the right are defined to be positive. (a)The thickness of the positive domain is a. (b)The thickness of the positive domain is b. It is easy to see that the two ASL are the same.

situations of Fig.2—10(a) and Fig.2—11(a) to Fig.2—10(b) and Fig.2—11(b). For resonators,these two situations are the same. From Figs.10, we can see that either one can be obtained by simply rotating the other by 180^0 about an axis perpendicular to the sheet. But for transducers, with a same ASL, two different transducers can be made as shown in

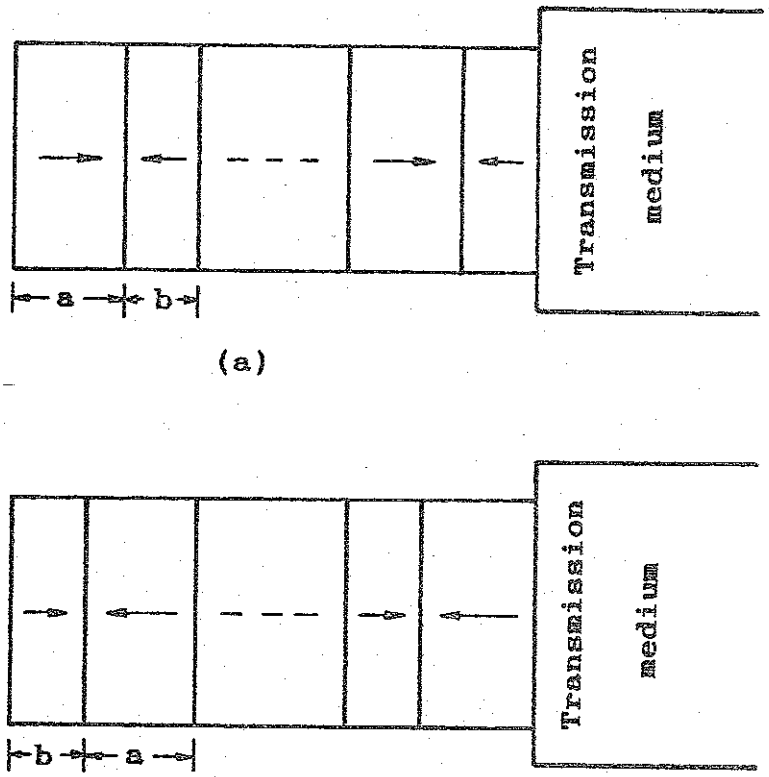

Fig.2—11.Schematic diagrams of transducers made of ASL(electrodes are omitted). Domains with their polarization directions towards the right are defined to be positive. The transmission medium is made of a single domain $LiNbO_3$ crystal. (a)The thickness of the positive domain is a. (b)The thickness of the positive domain is b. It is easy to see that the two ASL are the same, but the two transducers are different.

Figs.2—11. In Fig.2—11(a), the thickness of the domain in contact with the transmission medium is b, much smaller than that (thickness of a) in Fig.2—11(b). Obviously, these two situations are not the same and therefore the impedances of the two are different. But when a=b, there is no difference between these two situations as can be seen from Figs.2—11 and Eq.(2—24).

§2—4.Summary

We have analyzed theoretically the ultrasonic excitation and propagation in the ASL by the piezoelectric effect and deduced the expressions of electric impedances of both resonators and transducers. The resonance conditions show that there are two kinds of resonances existing in the ASL. One is the main resonance which is determined by the period of the ASL. This makes the ASL of potential applications in acoustic devices working at frequencies of several hundred megahertz to several gigahertz. The other one, the satellite-like resonance frequency,is related to the total thickness of the ASL. This phenomenon is similar to the satellite in x-ray or electron diffraction due to the existance of a super-structure. By adequate choice of the electrode area and the domain number, the radiation resistance or the real part of the impedance of the transducer made of the ASL can be made equal to or even larger than its reactance. The transducers thus fabricated will be very efficient.

Experimentally, we have prepared a set of resonators and transducers. Electric measurements verify our

predictions. Resonance frequencies up to 1000 MHz have been detected in the ASL with period of several microns. The satellite-like resonance phenomenon has been observed for the first time in acoustics. This phenomenon is not shared by transducers because of lack of the longer periodicity. Transducers with an insertion loss close to 0dB at 555 MHz have been made.

Discussions have been made about some interesting problems. In the long wavelength regime, the ASL behaves as if it were homogeneous. Eq.(2—17) (or 2—24) can be reduced to the familiar one for a resonator (or a transducer) made of a single domain crystal. But the physical parameters such as piezoelectric, dielectric coefficients are averaged. The acoustic power emitted by the ASL into the transmission medium is directly proportional to the square of the domain numbers. This makes the ASL much more preferable in practical applications. For the transducer, with a same ASL, two transducers with different impedances can be made respectively according to whether the thickness of the domain in contact with the transmission medium is a or b. This is due to the asymmetry of its boundary conditions. This should be kept in mind when one prepares the sample, especially if the difference between a and b is very large. Owing to the fact that the two faces of the transmission medium are parallel, the reflected signals interfere with the main signal and thus makes the reflection coefficient rippled. Therefore the electric characteristics of the transducer are affected. In practice, this should be avoided. The method to eliminate this effect is either to

tilt one face relative to the other or to coat some sound-absorbing material on the free surface of the medium. In short, there remains much to be done in future.

Appendix

Consider an acoustic wave propagating along a direction lying in the yz plane of a $LiNbO_3$ crystal. This problem may be approached by transforming the constitutive matrices to the rotated coordinate system. We assume that the propagating direction is $\hat{z}'$, which is a unit vector along the normal of domain walls of the ASL, and that the angle between the normal and the z axis is ϑ. Then the piezoelectric equations to be used here are

$$T_3'(\vartheta)=C_{33}'(\vartheta)S_3'+C_{34}'(\vartheta)S_4'-h_{33}'(\vartheta)D_3' \quad , \tag{2—A1}$$

$$T_4'(\vartheta)=C_{34}'(\vartheta)S_3'+C_{44}'(\vartheta)S_4'-h_{34}'(\vartheta)D_3' \quad , \tag{2—A2}$$

$$E_3'(\vartheta)=-h_{33}'(\vartheta)S_3'-h_{34}'(\vartheta)S_4'+(\varepsilon_{33}'(\vartheta))^{-1}D_3' \quad , \tag{2—A3}$$

here

$$C_{33}'(\vartheta)=n^4C_{11}^D+2m^2n^2(C_{13}^D+2C_{44}^D)+4mn^3C_{14}^D+m^4C_{33}^D \quad ,$$

$$C_{34}'(\vartheta)=-mn^3C_{11}^D-mn(m^2-n^2)(C_{13}^D+2C_{44}^D)-n^2(3m^2-n^2)C_{14}^D+m^3nC_{33}^D \quad ,$$

$$C_{44}'(\vartheta)=m^2n^2(C_{11}^D-2C_{13}^D+C_{33}^D)+2mn(m^2-n^2)C_{14}^D+(m^2-n^2)^2C_{44}^D \quad ,$$

$$h'_{33}(\vartheta)=mn^2(h_{31}+2h_{15})-n^3h_{22}+m^3h_{33}\ ,$$

$$h'_{34}(\vartheta)=m^2n(h_{33}-h_{31})-n(m^2-n^2)h_{15}+mn^2h_{22}\ ,$$

$$[\varepsilon'_{33}(\vartheta)]^{-1}=n^2(\varepsilon^s_{11})^{-1}+m^2(\varepsilon^s_{33})^{-1}\ ,$$

$m=\cos\vartheta$,$n=\sin\vartheta$.

For simplicity, we derive the electric impedance for a transducer with its either face fully matched to a semi-infinite transmission medium separately and a=b. Using the Green's function method we have get

$$Z=R-jX\ ,$$

$$R=\frac{2M_1v_1}{\omega^2A'_{12}}\tan^2[\frac{1}{2}k_1a]\ \sin^2k_1Na+\frac{2M_2v_2}{\omega^2A'_{12}}\tan^2[\frac{1}{2}k_2a]\ \sin^2k_2Na\ ,$$

$$X=-\left\{\frac{4NM_1v_1}{\omega^2A'_{12}}\tan\frac{1}{2}k_1a+\frac{M_1v_1}{\omega^2A'_{12}}\tan^2[\frac{1}{2}k_1a]\ \sin[2k_1Na]\right.$$

$$\left.+\frac{4NM_2v_2}{\omega^2A'_{12}}\tan\frac{1}{2}k_2a+\frac{M_2v_2}{\omega^2A'_{12}}\tan^2[\frac{1}{2}k_2a]\ \sin[2k_2Na]\right\}$$

$$+\frac{1}{\omega A'_{12}}\left\{M_1d+M_2d-\frac{C'_{44}(\vartheta)h'_{33}(\vartheta)-C'_{34}(\vartheta)h'_{34}(\vartheta)}{C'_{33}(\vartheta)C'_{44}(\vartheta)-C'^2_{34}(\vartheta)}\ h'_{33}(\vartheta)d\right.$$

$$-\frac{C'_{33}(\vartheta)h'_{34}(\vartheta)-C'_{34}(\vartheta)h'_{33}(\vartheta)}{C'_{33}(\vartheta)C'_{44}(\vartheta)-C'^{2}_{34}(\vartheta)}\,h'_{34}(\vartheta)d\Big\}$$

$$+\frac{d}{\omega\varepsilon'_{33}(\vartheta)A'_{12}}\,, \qquad (2\text{—}A4)$$

here

$d=2Na$,

A'_{12} is the electrode area,

$$v_1^2=\left\{C'_{33}(\vartheta)+C'_{44}(\vartheta)-\sqrt{[C'_{33}(\vartheta)-C'_{44}(\vartheta)]^2+4C'^{2}_{34}(\vartheta)}\right\}/2\rho\,,$$

$$v_2^2=\left\{C'_{33}(\vartheta)+C'_{44}(\vartheta)+\sqrt{[C'_{33}(\vartheta)-C'_{44}(\vartheta)]^2+4C'^{2}_{34}(\vartheta)}\right\}/2\rho\,,$$

$$M_1=\left\{h'_{33}(\vartheta)-\frac{C'_{33}(\vartheta)-\rho v_1^2}{C'_{34}(\vartheta)}\,h'_{34}(\vartheta)\right\}$$

$$\times\frac{[C'_{33}(\vartheta)C'_{44}(\vartheta)-C'^{2}_{34}(\vartheta)]\,h'_{33}(\vartheta)-[C'_{44}(\vartheta)h'_{33}(\vartheta)-C'_{34}(\vartheta)h'_{34}(\vartheta)]\,\rho v_2^2}{\rho(v_1^2-v_2^2)[C'_{33}(\vartheta)C'_{44}(\vartheta)-C'^{2}_{34}(\vartheta)]}$$

$$M_2=\left\{h'_{33}(\vartheta)-\frac{C'_{33}(\vartheta)-\rho v_2^2}{C'_{34}(\vartheta)}\,h'_{34}(\vartheta)\right\}$$

$$\times\frac{-[C'_{33}(\vartheta)C'_{44}(\vartheta)-C'^{2}_{34}(\vartheta)]\,h'_{33}(\vartheta)+[C'_{44}(\vartheta)h'_{33}(\vartheta)-C'_{34}(\vartheta)h'_{34}(\vartheta)]\,\rho v_1^2}{\rho(v_1^2-v_2^2)[C'_{33}(\vartheta)C'_{44}(\vartheta)-C'^{2}_{34}(\vartheta)]}$$

References of chapter 2:

1.Y.Y.Zhu, N.B.Ming, W.H.Jiang, and Y.A.Shui, Appl.Phys.Lett., 53, 2278 (1988).

2.Y.Y.Zhu, N.B.Ming, W.H.Jiang, and Y.A.Shui, Appl.Phys.Lett., 53, 1381 (1988).

3.H.E.Bommel, and K.Dransfeld, Phys.Rev.117, 1245 (1960).

4.R.F.Mitchell, Philips Res.Suppl.3, 1 (1972).

5.D.A.Berlincourt, D.R.Curran, and H.Jaffe, in Physical Acoustics, edited by W.P.Mason(Academic, New York, 1964), Vol.1A, p.169.

6.W.R.Smith, H.M.Gerard, J.H.Collins, T.M.Reeder, and H.J.Shaw, IEEE Trans.Microwave Theory and Tech., MTT-17, 856 (1969).

7.A.H.Meitzler, and E.K.Sittig, J.Appl.Phys.40, 4341 (1969).

8.B.A.Auld, Acoustic Fields and Waves in Solids (Wiley-Interscience, New York, 1973), Vol.1, p.272.

9.J.DeKlerk, in Proceedings of the International School of Physics "Enrico Fermi", Vol.63, A Physical Approach to Elastic Surface Waves, edited by D.Sette (North-Holland, Amsterdam, 1976), p.437.

10.E.K.Sittig, in Progress in Optics Vol.10, Elatstooptic Light Modulation and Deflection, edited by E.Wolf (north-Holland, Amsterdam, 1972), p.231.

11.A.V.Turik, and E.I.Bondarenko, Ferroelectrics 7, 303 (1974).

CHAPTER 3

Piezoelectric effect of quasiperiodic acoustic superlattice[1]

The self-similarity is a major feature of quasiperiodic superlattices. There are many theoretical works devoted to it in the literature[2]. Its experimemtal verification is mainly performed by x-ray and Raman scattering measurements[3,4], where the self-similarity is not so obvious. For example, in Raman scattering measurements, the inelastic scattering dips, which reflect the properties of the reciprocal space, are superimposed on the elastic scattering peak. Only a few are discernible. Thus many interesting information of the reciprocal space is lost. In this chapter, we provide a new experimental method of revealing the special characteristics of quasiperiodic superlattices. The spectrum of ultrasonic waves excited in a Fibonacci acoustic superlattice (FAS, one type of quasiperiodic structures) contains much more information. Not only the stronger resonant peaks but also many weaker peaks are detected[1]. They can all be indexed by a certain rule. The self-similarity are clear at a glance.

§3—1.Theory

As mentioned in chapter 2, the acoustic superlattice(ASL) can be viewed as a structure composed of a series of sound δ-sources arranged periodically or quasiperiodically. These δ-sources are generated by the discontinuity of the piezoelectric stress which is the product of piezoelectric coefficient and electric field. So

there are two ways to prepare a periodic or quasiperiodic ASL. The first one is to use piezoelectric crystals such as a $LiNbO_3$ single crystal with periodic or quasiperiodic laminar ferroelectric domain structures induced by the growth striations(Fig.3—1 and 3—2)[5—8]. The sign of piezoelectric coefficient of the layered crystal changes alternately. In this case, the piezoelectric coefficient is discontinuous at the ferroelectric domain boundaries which become sound sources under the action of an alternating external electric field and the excited acoustic waves are bulk waves. The second one is to fabricate an interdigital surface-wave transducer with electrode intervals varying periodically or quasiperiodically(Fig.3—3 and 3—4). The transducers are easily fabricated by standard photolithographic technique[9,10]. Aluminum electrodes are deposited on a piezoelectric substrate such as a single domain crystal of $LiNbO_3$. When an alternating external voltage is applied onto the electrodes, an electric field is built beneath the surface of the substrate as shown in Fig.3—3(b) and Fig.3—4(b), which can be simplified to Fig.3—3(c) and 3—4(c)[11]. The electric field generated beneath the surface of the substrate alternates its sign periodically or quasiperiodically. In this case, the electric field is discontinuous on the bisect line of each electrode beneath the surface of the substrate which is also a sound source and the excited acoustic waves are surface-waves.

In both cases, the physical mechanism of ultrasonic excitation is obvious. According to Bommel and Dransfeld[12],

under the action of an external electric field, the discontinuity in piezoelectric stress at the ferroelectric domain boundaries (or on the bisect line of each electrode beneath the surface of the substrate) must be balanced by a strain $S(u_m)$. Here u_m represents the position where the discontinuity takes place. This strain will propagate as an acoustic wave

$$S(u)=S(u_m)\cos(\omega t-ku). \qquad (3—1)$$

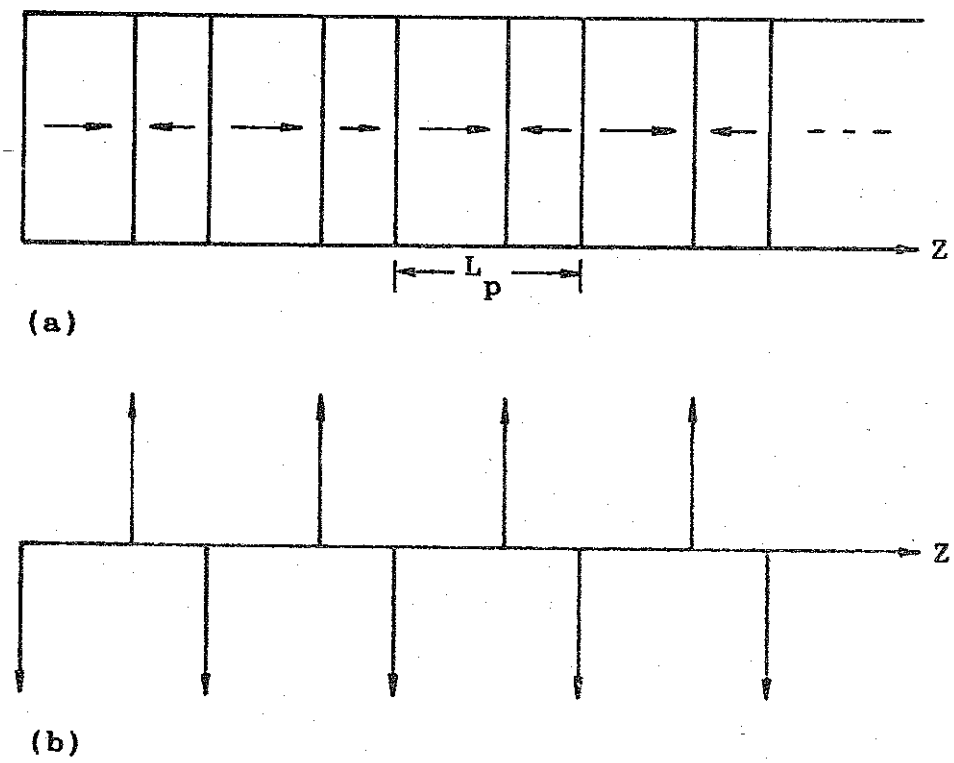

Fig.3—1.(a)Schematic diagram of periodic ASL with the periodicity of L_p (the arrows indicate the directions of the spontaneous polarization). (b)Corresponding sound δ sources.

So each domain boundary(or the bisect line of each electrode

where the discontinuity of electric field takes place)can be viewed as a sound δ-source(see Figs.3—1(b), 3—2(b), 3—3(d) and 3—4(d)).

Because of this similarity, in what follows, we will limit ourselves to $LiNbO_3$ crystals with quasiperiodic laminar ferroelectric domain structures. The results obtained will suit each other.

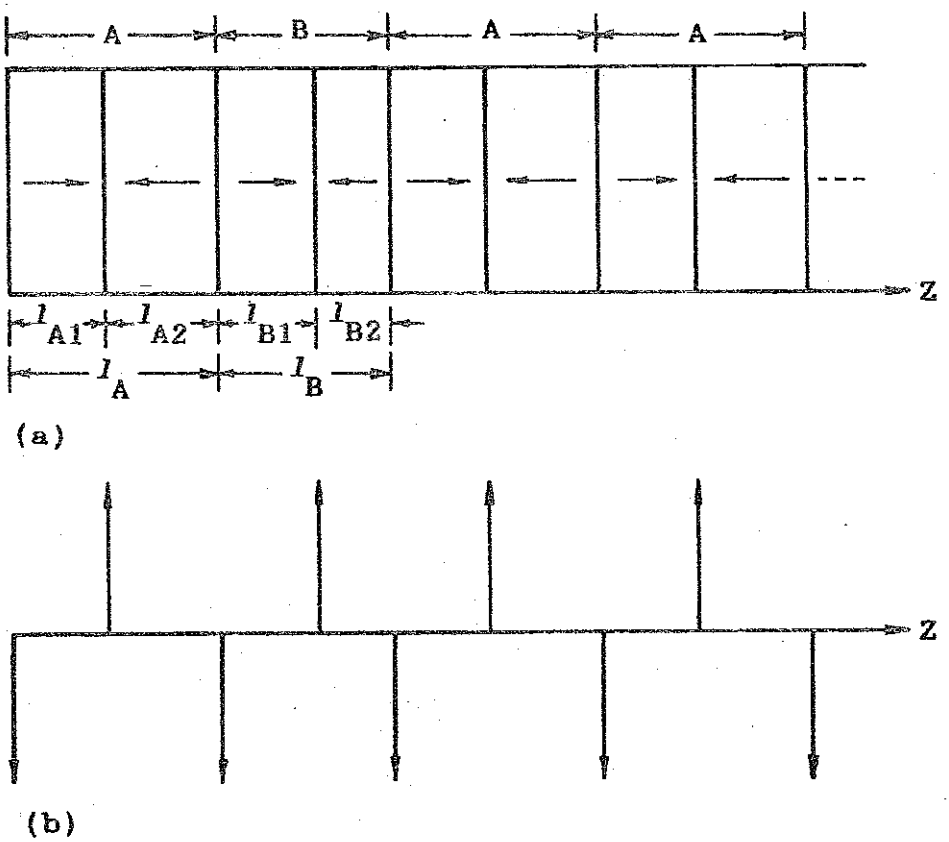

Fig.3—2.Fibonacci ASL of $LiNbO_3$ crystals. (a)Schematic diagram of the superlattice. (b)Corresponding sound δ sources.

Here we choose $l_{A1}=l_{B1}=l$ and $l_A=\tau l_B$ with $l_A=l_{A1}+l_{B1}$, $l_B=l_{B1}+l_{B2}$ as shown in Fig.3—2(a). In addition, we assume

that the lateral dimensions of the FAS are much larger tha the width of the ferroelectric domains and that the norma

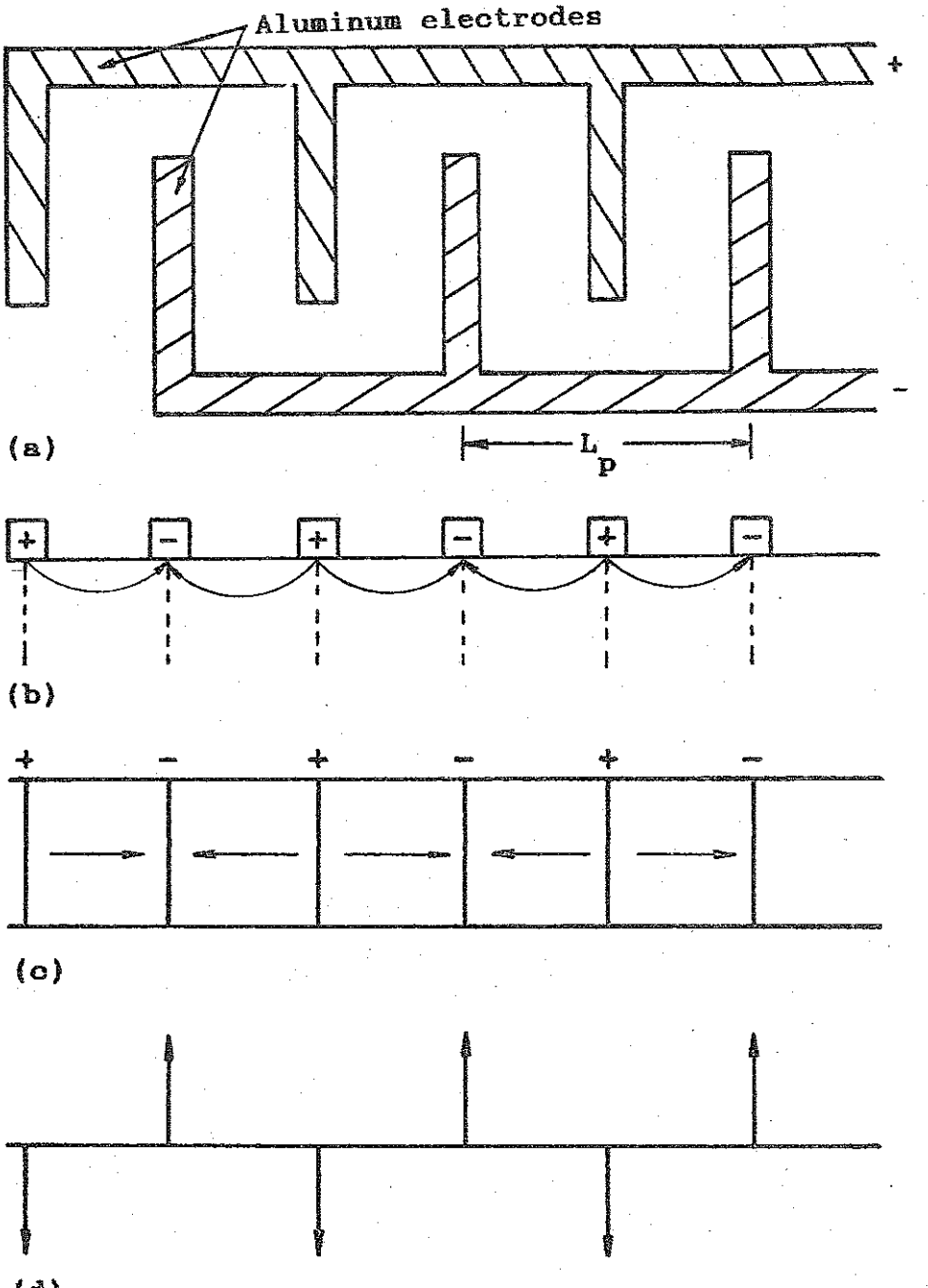

Fig.3—3.(a)Periodic interdigital transducer schemati diagram with the periodicity of L_p. (b) Side view of th interdigital transducer, showing electric field pattern

inside the thin skin of the substrate. (c)Electric field viewed from top. (d)Corresponding sound δ sources.

of the domain boundaries coincides with the z axis, then the one dimensional model is applicable. Under these conditions, when an alternating voltage applied on the {0001} faces of the sample, a longitudinal planar wave propagating along the z axis will be excited inside the superlattice. It obeys the wave equation

$$\frac{\partial^2 u_3}{\partial z^2}-\frac{1}{v^2}\frac{\partial^2 u_3}{\partial t^2}=\frac{2h_{33}{}^D_3}{C^D_{33}}\sum_m(-1)^m\delta(z-z_m), \qquad (3—2)$$

where u_3 represents the particle displacement in the z direction, v is the sound velocity. $\{z_m\}$ are the positions of the ferroelectic domain boundaries.

Eq.(3—2) is a fundamental wave equation governing the excitation and propagation of sound wave in an ASL. The term on the right-hand side stands for the exciting source of the sound wave. As above mentioned, the ultrasonic waves in such a superlattice are excited by a series of δ-sources at the domain boundaries, which is also shown in Eq.(3—2). Therefore, we can make use of the impulse response model[9,10] to obtain the ultrasonic spectrum excited by the FAS of $LiNbO_3$ crystals.

As can be seen in Fig.3—2(b), the δ-sources can be divided into two parts,one for positive δ-sources, the other for negative δ-sources. Each forms a Fibonacci sequence. The negative is displaced a distance l relative to the

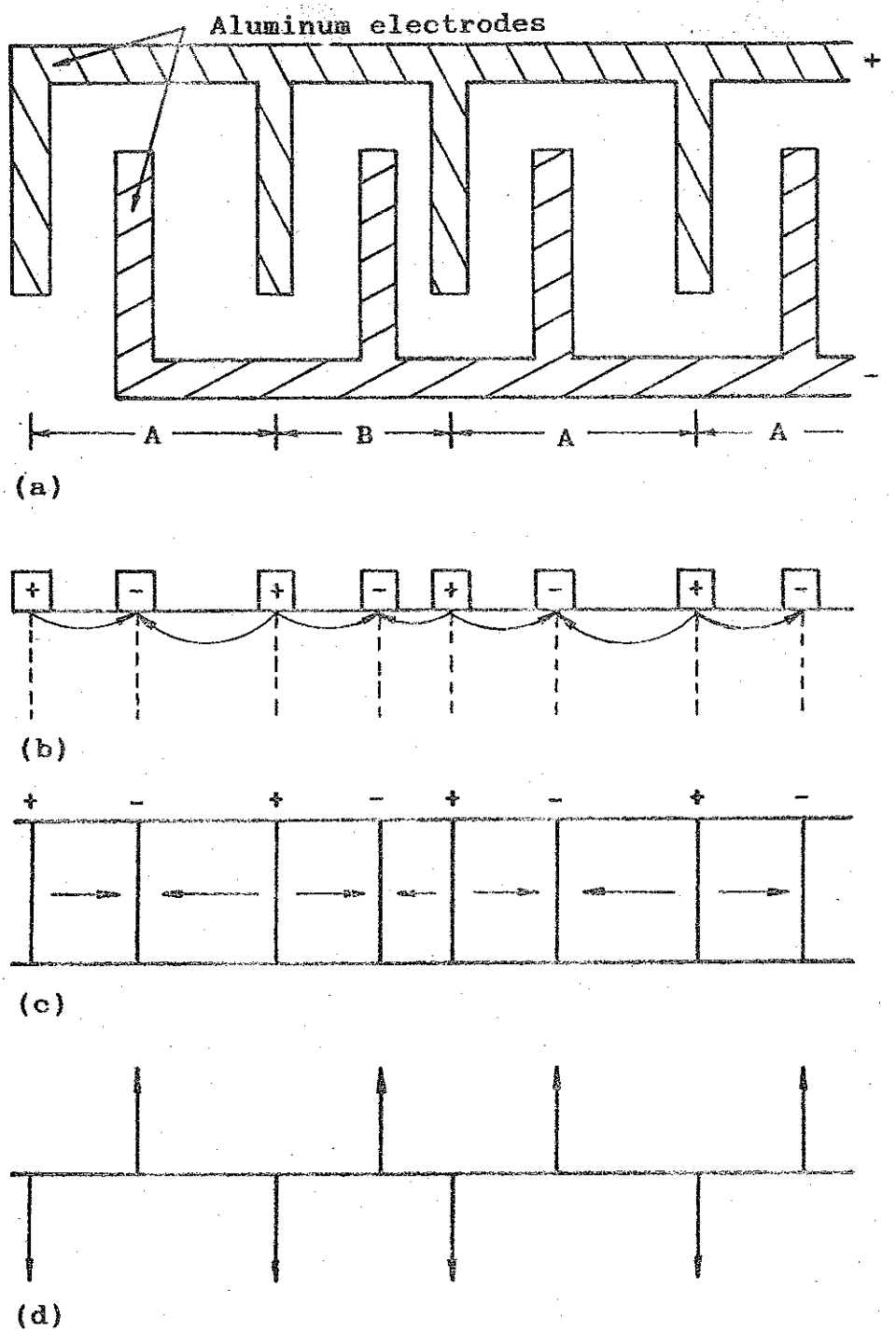

Fig.3—4.(a)Quasiperiodic interdigital transducer schematic diagram. (b)Side view of the interdigital transducer, showing electric field patterns inside the thin skin of the substrate. (c)Electric field viewed from top.

positive. Performing Fourier transforms on the positive terms and the negative terms on the right-hand side of Eq.(3—2) separately, and adding them together, we can get the ultrasonic spectrum for an infinite array, which is

$$H(k)\propto\sum_{m,n}\sin\frac{1}{2}kl\ \ e^{i(\frac{1}{2}kl-X_{m,n})}\frac{\sin X_{m,n}}{X_{m,n}}\delta(k-G_{m,n}), \qquad (3—3)$$

where k is the wave vector. In deriving Eq.(3—3), the projection method has been used[13,14]. The appearance of the term $\sin(kl/2)$ is due to the relative displacement between the positions of positive δ-sources and that of negative δ-sources.

§3—2.Experiments and discussions

The resonant peaks in the ultrasonic spectrum can be obtained from the δ-functions in Eq.(3—3), which is $k=G_{m,n}=2\pi(m+n\tau)/D$, or

$$f_{m,n}=v(m+n\tau)/D, \qquad (3—4)$$

where m, n are integers. Here $G_{m,n}$ is the reciprocal vector of the Fibonacci superlattice. So indexing the resonant peaks in ultrasonic spectrum is equivalent to indexing the reciprocal space. The most significant resonant peaks in ultrasonic spectrum occur at $f=f_{m,n}$ for which $X_{m,n}$ is small. This means that n/m must be close to τ. It is well known

that the best rational approximants to τ occur when m and n are successive Fibonacci integers[15], $(m,n)=(F_{p-1}, F_p)$, where $F_{p+1}=F_p+F_{p-1}$ and $(F_0,F_1)=(0,1)$. For these values of (m,n), $f_{m,n}$ takes the form of (integer)$\times v\tau^p/D$ and these resonant peaks are labeled τ^p.

The results are much similar to that of acoustic-phonon transmission[16] except for the substitution of $f_{m,n}=v(m+n\tau)/D$ for $f_{m,n}=v(m+n\tau)/2D$ and of peaks for dips. These can be explained as follows. In the case of excitation of ultrasonic waves, if the piezoelectric medium is a superlattice one, the ultrasonic waves will be excited on the ferroelectric domain boundaries. The waves coming from successive boundaries will interfere with each other. Those satisfying the constructive interference will appear as resonant peaks in the ultrasonic spectrum. Whereas in the case of acoustic-phonon transmission, when the phonons, reflected from successive interfaces, satisfy the constructive interference, they will appear as dips in transmission spectrum. Obviously, the peaks in the former case just correspond to the dips in the latter case. The occurrence of the factor 1/2 in the expression for dip frequencies is due to the fact that the path difference between phonons reflected from the adjacent interfaces is twice as large as the path difference between the ultrasonic waves excited on the adjacent ferroelectric domain boundaries.

We have calculated the ultrasonic spectrum excited by the FAS numerically. In order to be compared with the experiments, only the ultrasonic spectrum of the

superlattice of the eighth Fibonacci generation has been shown in Fig.3—5(a), with the parameters selected to be in line with experiments. It is worth noting that the resonant peaks obey the Eq.(3—4). In this figure, several frequencies predicted by expression $f=f_{m,n}=(m,n)$ are indexed. As expected, the main peaks are observed at $f_{m,n}$ for which m and n are neighboring Fibonacci numbers, as indicated by τ^p.

Detailed calculations have shown that the resonant peaks densely fill reciprocal space in a self-similar manner. It is just expected. It is well known that the self-similarity exists in the spectra of phonon[16-20], electron energy[19], polariton[21] and in X-ray diffraction[3], etc. Here again, in the ultrasonic spectrum excited by the FAS of $LiNbO_3$ crystals, the self-similarity also exists. It may be said that the self-similarity is a common feature of the Fibonacci superlattices and is a reflection of the self-similar structure of Fibonacci superlattices in reciprocal space.

Experimentally, we have fabricated several quasiperiodic surface-wave interdigital transducers of the eighth Fibonacci generation. Aluminum electrodes are deposited on the surface of a single domain crystal of $LiNbO_3$. The intervals between the electrodes varied successively according to the Fibonacci sequence. In this case, the surface wave velocity v=3944m/sec. The other parameters are l=39.0μm, l_B=62.3μm and l_A=100.8μm. The ultrasonic spectra are measured, which is the ratio of output voltage to input voltage. In the measurement, the

frequency scan range of the Hp8505 network analyzer is selected to be from 12.2 to 82.2MHz. The output voltage signals which satisfy the resonant conditions, i.e., $f_{m,n}=v(m+n\tau)/D$, are strengthened. The others are diminished. Figs.3—5(b) and (c) show one of these results. In the ultrasonic spectrum many sharp peaks appear at nonequal intervals. It is clear that there exists a one-to-one correspondence between the resonant peaks in Fig.3—5(a) and 3—5(b) or 3—5(c). Table 3—1 shows the results calculated and measured. The agreement is quite satisfactory.

In Fig.3—5 only some much stronger resonant peaks have been indexed. More recently, L.X.Zhang et al.[22] have pointed out that the whole reciprocal space can be indexed by a certain rule. They proved that the reciprocal space can be divided into equivalent intervals. Choose an appropriate reduced interval and index the reciprocal vectors in it. Then multiplying them by τ^p(p is an integer), they have indexed all the other vectors.

Here it should be mentioned that although the extinction phenomenon, which will be discussed in the next chapters, also exists in the ultrasonic spectrum, it is difficult to detect because the modes of the bulk wave[23] always appear in the region where the mode (2,2) appears. Experimentally, we have observed that above 82.2MHz, the resonant peaks are rather chaotic.

In order to compare the ultrasonic spectrum of the FAS with that of the periodic ASL, Figs.3—6(a) and (b) shows the theoretical and the experimental ultrasonic spectra obtained from a periodic ASL of $LiNbO_3$ crystal. The analysis

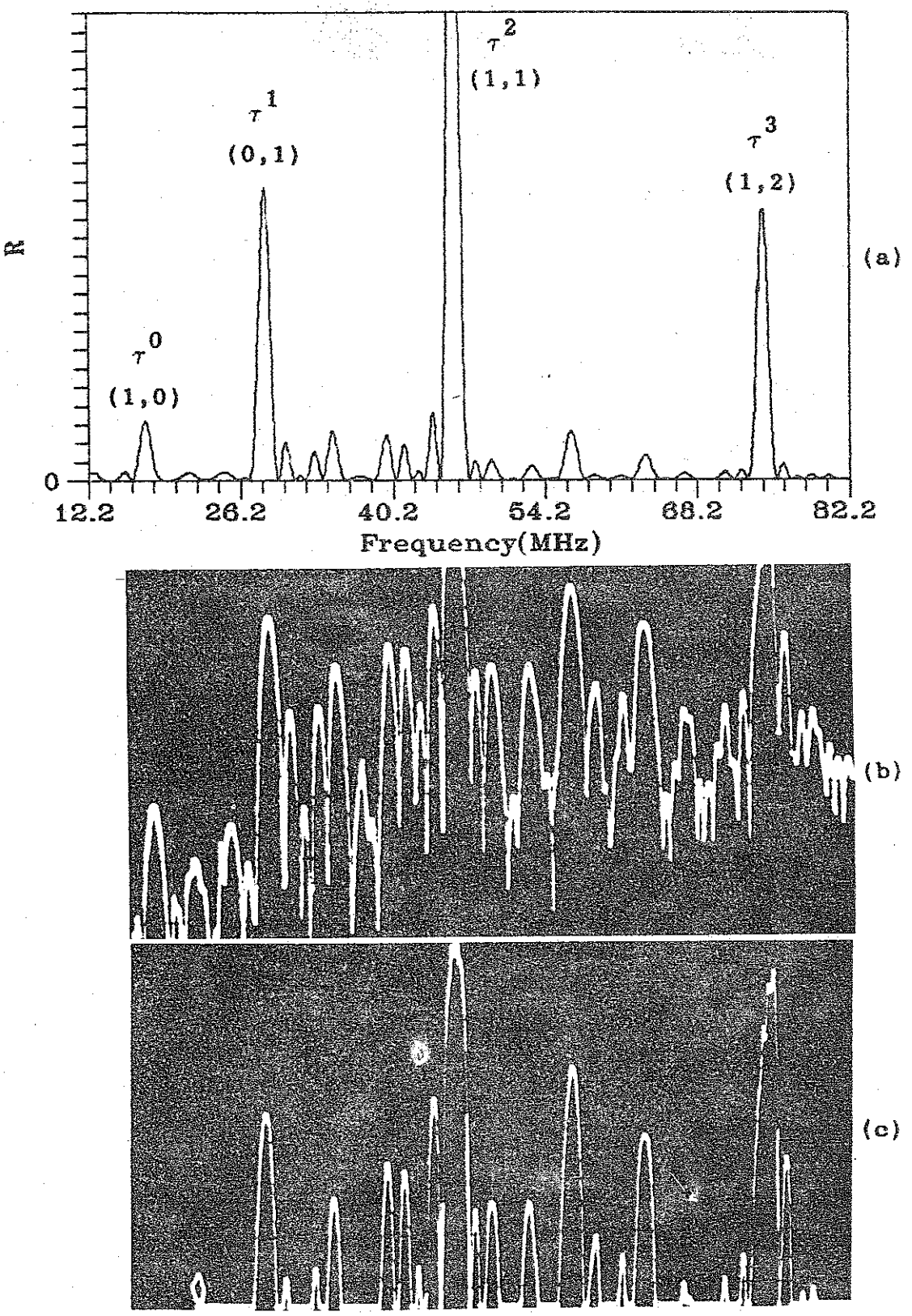

Fig.3—5.Ultrasonic spectrum for an eigth-generation

Fibonacci acoustic superlattice. (a)Ultrasonic spectrum calculated for a $LiNbO_3$ crystal. R, relative value of radiation resistance. (b)Ultrasonic spectrum measured. (c)The same as (b) with the amplitude magnified. In both (b) and (c) the amplitude is in logarithmic scale.

Table 3—1.Comparison between resonance frequencies calculated and measured for a quasiperiodic surface-wave interdigital transducer.

Vibrational mode	Resonance frequency f(MHz)	
(m,n)	cal.	mes.
(1,0)	17.5	17.5
(0,1)	28.3	28.4
(1,1)	45.8	45.8
(1,2)	74.1	74.5

and the experiment are analogous to our previous work[24,25]. The resonant frequency measured is 550 MHz, close to the theoretical one, 553 MHz, which is calculated from $f=v/L_p$ with $L_p=13.2\mu m$ and v=7300m/sec. Here L_p is the periodicity of the periodic ASL. Obviously Figs.5 and 6 bear no resemblance to each other.

§3—3.Summary

We have studied and obtained some of the features of the ultrasonic spectrum excited by an FAS. Two ways to fabricate such a superlattice are presented. The ultrasonic spectrum is excited by piezoelectric effect. Not only the

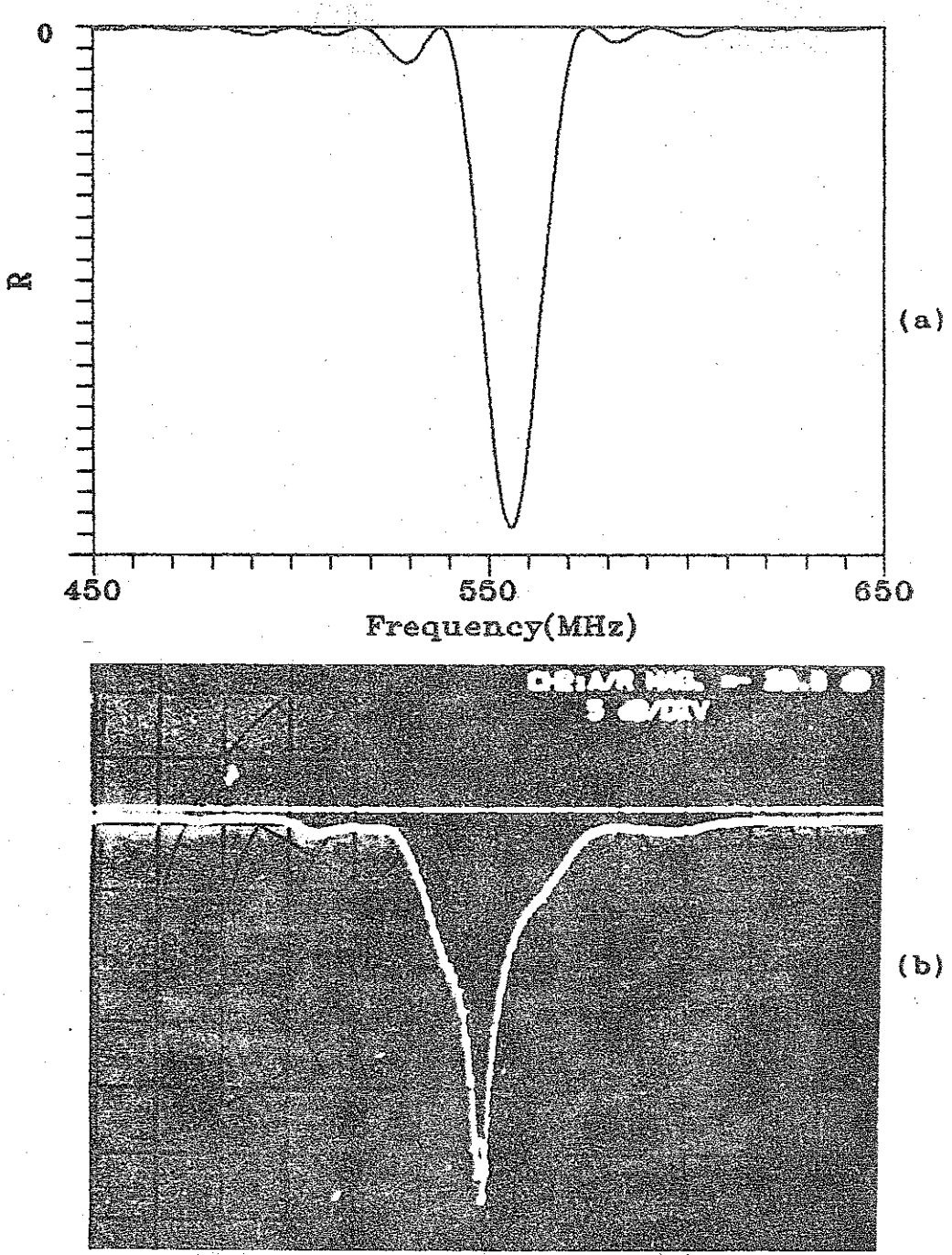

Fig.3—6.Ultrasonic spectrum for a periodic acoustic superlattice of a $LiNbO_3$ crystal. (a)Ultrasonic spectrum calculated. R, relative value of radiation resistance. (b)The spectrum measured which is represented by the reflection coefficient. The horizontal scale is frequency

centered at 550MHz with a scan width Δf=200MHz.

stronger resonant peaks but also many weaker peaks are detected experimentally. The self-similar structure of the spectrum is verified satisfactorily.

References of chapter 3:

1.Y.Y.Zhu, N.B.Ming, and W.H.Jiang, Phys.Rev.B40, 8536 (1989).

2.P.J.Steinhardt, and S.Ostlund, The Physics of quasicrystals (World Scientific, Singapore, 1987).

3.R.Merlin, K.Bajema, R.Clarke, F.Y.Juang and P.K.Bhattacharya, Phys.Rev.Lett.55, 1768 (1985).

4.M.W.C.Charma-wardana, A.H.MacDonald, D.J.Lockwood, J.M.Baribeau, and D.C.Houghton, Phys.Rev.Lett.58, 1761 (1987).

5.N.B.Ming, J.F.Hong and D.Feng, J.Mater.Sci.27, 1663 (1982).

6.N.B.Ming, J.F.Hong, Z.M.Sung and Y.S.Yang, Acta Phys.Sin.(in Chinese) 30, 1672 (1981).

7.J.F.Hong, and Y.S.Yang, Acta Opt.Sin. (in Chinese) 4, 821 (1986).

8.A.Feisst and P.Koidl, Appl.Phys.Lett.47, 1125 (1985).

9.R.H.Tancrel and M.G.Holland, Proc.IEEE.59, 395 (1971).

10.C.S.Hartmann, D.T.Bell, JR.and R.C.Rosenfeld, IEEE.Trans.SU-20, 80 (1973).

11.W.R.Smith, H.M.Gerard, J.H.Collins, T.M.Reeder and H.J.Shaw, IEEE.Trans.MTT-17, 856 (1969).

12.H.E.Bommel and K.Dransfeld, Phys.Rev.117, 1245 (1960).